Prediction of the cutting forces during turning of Titanium Alloy Ti6Al4V

[1]Ishankumar Upadhyay, [2] Pankaj Rathod, [3] Krishna Tadvi
[13]ME Student,[2]Associate Professor
Mechanical Engineering Department
L.D.College of Engineering, Ahmedabad

***Abstract* – High strength, low density, and excellent corrosion resistance are the main properties that make titanium alloys favoured for a variety of applications. In spite of its fascinating characteristics, it is considered to be difficult to machine material because of its low thermal conductivity (resulting in high heat generation at the chip-tool interface), high chemical reactivity-especially at high cutting temperature (leading to an accelerated adhesive tool wear) and low modulus of elasticity (causing harmful deflections in the workpieces). The titanium alloy Ti6Al4V is very difficult to machine and machinability criteria like; cutting force, friction force, surface roughness and tool life etc are very important parameters to consider. Mathematical model has generated to predict cutting forces during the machining of Ti6Al4V. The results are in very good agreement with the experimental data.It proves the potentiality of the oxley's model to use for titanium alloy Ti6Al4V.**

***Index Terms* – Titanium alloys,Difficult to cut materials, Cutting forces, machinability,Oblique cutting**

1.INTRODUCTION

Titanium alloy (Ti-6Al-4V) has a chemical composition of 6% aluminium, 4% vanadium, 0.25% (maximum) iron, 0.2% (maximum) oxygen and the remainder titanium.Ti6Al4V is a material having a high mechanical strength, corrosion and creep resistance, and high strength-to-weight ratio, which make it an attractive material for various industries such as automotive, aerospace, power generation, and biomedical industries. However, these superior properties as well as its low thermal conductivity and chemical reactivity make it a challenge to machine Ti-6Al-4V at optimal conditions. [1]
The properties of Titanium alloy are summarised as follows:

Physical Properties	
Density	4.43 g/cc
Mechanical Properties	
Hardness	36 HRC
Tensile strength(Ultimate)	950 MPa
Tensile strength(Yield)	880 MPa
Modulus Of Elasticity	113.8 GPa
Compressive Yield Strength	950 MPa
Poisson's ratio	0.342
Thermal Properties	
Specific Heat Capacity	0.5263 KJ/g-˚C
Thermal Conductivity	6.7 W/m-k
Melting Point	1604-1607˚C

[a]

Table-1 Ti6Al4V properties

Ti6Al4V is known as the "workhorse" of the titanium industry because it is by far the most common Ti alloy, accounting for more than 50% of the titanium usage. It is an alpha + beta alloy that is heat treatable to achieve moderate increase in strength.

In spite of its fascinating characteristics, it is considered to be difficult to machine material because of its low thermal conductivity (resulting in high heat generation at the chip-tool interface), high chemical reactivity-especially at high cutting temperature (leading to an accelerated adhesive tool wear) and low modulus of elasticity (causing harmful deflections in the workpieces). (Komanduri and Hou 2002). Siekmann (1955) pointed out that 'machining of titanium and its alloys would always be a problem, no matter what techniques are employed to transform this metal into chips'.[1]

2. EXISTING LITERATURE

E.O.Ezugwu et al.[2] presented a paper on "the machinability of an aeroengine alloys", reported that titanium alloys are usually machined with uncoated straight grade cemented carbide (WC-Co) tool at higher cutting speeds in excess of 45 m/min. Machining at higher speed conditions tend to generate higher temperature close to the tool nose resulting in excessive stresses at the tool nose causing plastic deformation and subsequent tool failure.

At interfacial temperatures of 500˚C and above, titanium and its alloys are very reactive with cutting tool materials, at such high temperature conditions titanium atoms diffuse into the carbide tool material and react chemically with carbon present in the tool to form an interlayer of titanium carbide (TiC) which bonds strongly to both tool and the chip to form a seizure zone, consequently

minimising diffusion wear mechanism. The separation of welded junction results in tool material being carried away by the fast flowing chip.

D. C. Drucker [3] analysed the Mechanics of Metal Cutting, The influences of speed of cutting, depth of cut, and rake angle were correlated by the consideration of dynamic plasticity. The effect of non-homogeneity of the material had been analyzed and shown to account for the gradual change from the discontinuous to the continuous type of chip as the cutting speed is increased, and for the marked increase in the specific cutting force as the depth of cut decreased.

H T Young et al. [4] explained that the first step in making accurate predictions of cutting forces is to make accurate predictions of the direction of chip flow. Their investigation has been limited to tools having a zero inclination angle and zero normal rake angle.Undeformed chip section bounded by cutting edge of arbitrary shape makes an angle Θ with positive X axis as shown in Fig.1.

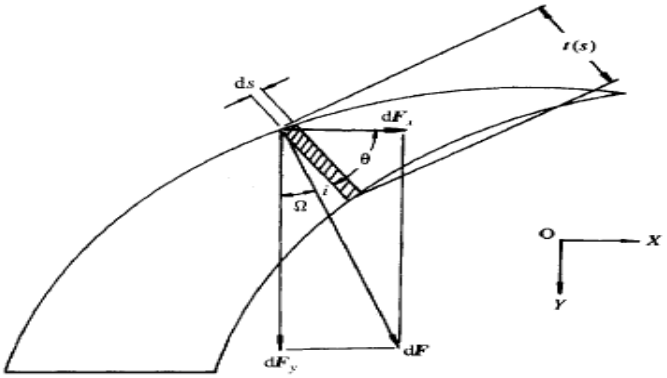

Fig.1 Resolution of differential friction force at nose radius edge into components in a set of reference directions at right angles [3]

Below mentioned formula used to predict the chip flow angle described as;

$$\bar{\Omega} = \tan^{-1}\left(\frac{F_x}{F_y}\right) = \tan^{-1}\left(\frac{\int \sin\Omega dA}{\int \cos\Omega dA}\right)$$

A Vyas at al. [5] reported that saw tooth chip normally occurs during the machining of very hard brittle material like Ti6Al4V.Two theories for the origin of saw tooth chip were proposed. In first theory, it was assumed that they are of thermal origin while other theory assumed that saw chip arises due to periodic development of the crack in the original surface of the work. The following conclusions were arrived at;

1) An increase in cutting speed has opposing effects: an increase in the tendency for saw-tooth chip formation due to increased strain rate, but a decrease due to thermal softening.
2) Two types of cracks are involved in saw tooth chip formation:
   - Gross cracks that are continuous across the chip width
   - Microcracks that are discontinuous across the chip width

J. Wang [6] worked on "Development of a chip flow model for turning operations", A model was presented which predicts the chip flow direction in turning operations with nose radius tools under oblique cutting conditions, The model has been prepared by using tool cutting edge geometry and the cutting conditions (feed and depth of cut). The undeformed chip section is separated into two regions, region A and B corresponding to the nose radius edge and straight part of main cutting edge respectively. In the model two cases have been taken as shown in Fig.2.35 a) when d' > r(1-Sin Cs') and b) d' > r(1-Sin Cs') in which d' is the projection of depth of cut d and Cs'is the projection of approach angle Cs. Chip flow angle increased with increase in inclination angle and feed rate and with a decrease in approach angle and normal rake angle.

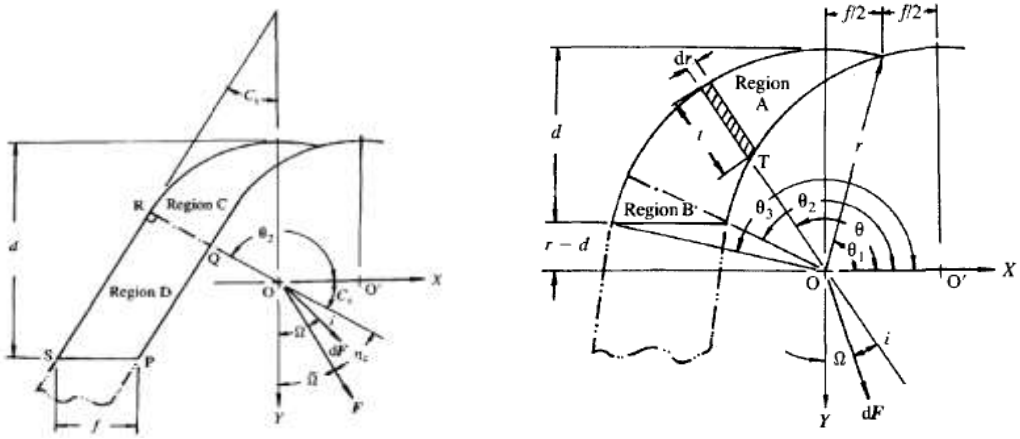

Fig. 2. case a) d' > r(1-sinCs') and case b) d' <= r(1-sinCs') [6]

Jiang Hua et al. [7] worked on "Prediction of chip morphology and segmentation during the machining of titanium alloys", A new interpretation of chip segmentation based on an implicit, Lagrangian, non-isothermal rigid viscoplastic finite element simulation of orthogonal machining of Ti–6Al–4V in which a dynamic flow stress model based on high strain rate and high temperature, and a ductile fracture criterion based on the strain energy are applied to the crack initiation during the chip segmentation. This model was verified by comparison with experimental results. It had been observed that chip segmentation under high cutting speed (V_c=600 m/min) is similar to the cutting speed of 120 m/min, except that the connecting portion of the chips is thicker and the segmentation is closer at the higher speed. This indicates that the resistance to crack propagation to the tool tip direction increases with the cutting speed. All the above simulation results showed that the fracture is not initiated in the free surface of the chip**.**

Based on the analysis of the simulation following conclusions were made;

- Chip formation in the cutting of Ti–6Al–4V is strongly influenced by crack initiation and propagation which results in discontinuous or serrated chip morphology.
- When cutting Ti–6Al–4V at low cutting speed, the chip obtained is discontinuous, while at high cutting speed the chip obtained is serrated.

S.A.Iqbal et al. [8] proposed that tool chip contact length is an important parameter in machining, as it provides an indication of the size of area of interaction between the hot chip and the tool surface and hence the interface heat transfer zone. A model has been prepared to predict the tool chip contact length of AISI 1045 steel and Ti6Al4V for various cutting speeds.

- The linear equation defining the contact length for AISI 1045 for a wide range of cutting speeds is obtained as:
  $Lc=1.56h_2 + 0.09h_1$ (AISI 1045 steel)
- The linear equation defining the contact length for Ti6Al4V for a wide range of cutting speeds is obtained as:
  $Lc=1.15h_2 + 0.70h_1$ (Ti6Al4V)

Where h_1= Undeformed chip thickness (set by the feed rate in the depicted orthogonal turning)
h_2= Actual chip thickness

Mohammad Sima et al. [9] investigated the influence of material constitutive models and elastic–viscoplastic finite element formulation on serrated chip formation for modeling of machining Ti–6Al–4V titanium alloy. Temperature-dependent flow softening based modified material models have been proposed where flow softening phenomenon, strain hardening and thermal softening effects and their interactions has been coupled. Orthogonal cutting experiments have been conducted with uncoated carbide (WC/Co) and TiAlN coated carbide cutting tools. Temperature- dependent flow softening parameters are validated on a set of experimental data by using measured cutting forces and chip morphology. Finite Element simulations are validated with experimental results at two different rake angles, three different undeformed chip thickness values and two different cutting speeds.

Experimental results suggested that the cutting forces increased with increase in cutting speed and thrust forces decreased with decreasing rake angle. Flow softening is most effective between 300and700˚C and causes adiabatic shearing in the deformation zone during machining of Ti–6Al–4V alloy much lower than allotropic phase transformation (b-transus) temperature. Flow softening increases the degree of chip serration chip but produce more curved chips since strain-hardening effect weakens.

Guang Chen et al. [10] worked on the finite element simulation of high speed machining of Ti-6Al-4V based on ductile failure model. The following observations were made

- At extremely high speed (v=1,200, 2,400, and 4,800 m/min) cutting simulation results indicate that the energy-based ductile failure FE model can give a good prediction of chip morphology and cutting forces under different cutting conditions.
- As the cutting speed increases, the segment valley and peek of the chip decrease, conversely, the segment pitch increases slightly with cutting speed. The dimensions of segment chip morphology increase with feed rate.
- In the range of HSM, relatively low cutting speed (v=170, 210, and 250 m/min) cutting experiments have been carried out to further validate the FE model. The predicted chip morphology and cutting forces agree well with the experimental results which shown that ductile failure criterion is suitable for titanium alloy in HSM simulation.

M. Calamaz et al. [11] studied about "Numerical analysis of chip formation and shear localisation processes in machining the Ti-6Al-4V", A thermo-visco-plastic model for the machined material and a rigid with thermal behaviour for the cutting tool were assumed for the prediction of the chip morphology and cutting parameters such as cutting forces, temperature and cutting pressure. The Johnson-Cook law has been modified and implemented in the FE model to introduce the strain softening effect. Finite element simulation results were compared with the experimental results. Best result was obtained when using a high value of the friction coefficient together with the introduction of a strain softening parameter of 0.11. Also the strain distribution into the simulated chip is in good agreement with the deformed microstructure of the chip obtained by experimental tests.

3. SUMMARY OF LITERATURE REVIEW AND RESEARCH GAP

Based on the extensive literature review, it can be said that the machining of a titanium alloy Ti6Al4V is always difficult because of high chemical reactivity with all the tool materials. It is always advisable that uncoated carbide tools are the best candidate for the machining of titanium alloy. During the machining, the cutting forces, friction force, wear rates are very high. so tool life is very less. An analytical force model has not been developed till date and hence an attempt has been made to develop such a model. Work in developing models for the machining of Ti-6Al-4V alloy in a scientific manner enables predicting the optimized set of input parameters for Ti-6Al-4V to achieve better machining conditions. This work thus can lead to improved quality and higher productivity.

4. MATHEMATICAL FORMULATION

4.1 Basic Geometric Relationship

Oxley [12] has represented a geometric model for metal cutting as shown in the Fig.3. The model assumes that plane strain, steady state conditions apply. The plane AB, near the centre of the zone in which the chip is formed and the tool/chip are both assumed to be the directions of maximum shear stress and maximum shear strain rate.

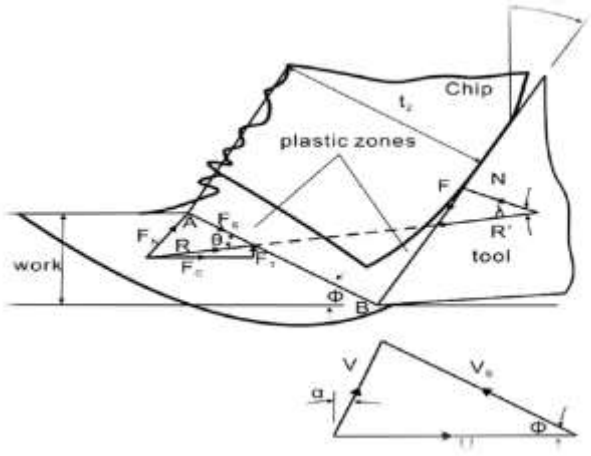

Fig 3 Oxley's Geometric Model For Metal Cutting [12]

In Fig 3 it is assumed that shear plane AB is to be a direction of maximum shear strain rate hence maximum shear stress with the shear strain rate constant along AB is described by

$$\bar{\gamma}_{ab} = \frac{cV_s}{L} \qquad \varepsilon'' = \frac{\bar{\gamma}_{ab}}{\sqrt{3}} \qquad \text{Eq.1}$$

4.2 Material modeling used in modeling

For Generalised Modeling approach material behaviour is to be known for under machining Condition. Johnson Cook material constitution model is used to represent the material flow stress as;

$$\sigma = (A + B\varepsilon^n)(1 + C\ln(\frac{\dot{\varepsilon}}{\varepsilon_o}))\,(1 - (\frac{T-T_r}{T_m-T_r})^m) \qquad \text{Eq.2}$$

Table 2 Johnson Cook model parameter for Ti6Al4V is taken as [13]

A(MPa)	B(MPa)	C	n	m
1098	1092	0.014	0.93	1.1

4.3 Calculation of the Shear Plane Temperature

As pointed out by the Abidi et al. [14] the temperature at the midpoint of the shear plane is calculated by equating the fraction β of the total plastic work done up to the mid plane of the primary shear zone. The energy expended is utilised to increase the temperature of the material.

For the Johnson-Cook material model the temperature of the shear plane T_{AB} is found from,

$$\int_{T_w}^{T_{AB}} \frac{\rho C_p T}{1-(\frac{T-T_r}{T_m-T_r})^m} dT = (1-\beta)(A\,\varepsilon_{AB} + \frac{B}{n+1}\varepsilon_{AB}^{n+1})(1+C\ln\frac{\dot{\varepsilon_s}}{\dot{\varepsilon_0}}) \qquad \text{Eq.3}$$

The partition coefficient β is assumed to be constant and evaluated at T_w.The temperature of the upper part of the shear zone T_{EF} can be obtained in a similar manner as,

$$\int_{T_w}^{T_{EF}} \frac{\rho C_p T}{1-(\frac{T-T_r}{T_m-T_r})^m} dT = (1-\beta)(A\,\varepsilon_{EF} + \frac{B}{n+1}\varepsilon_{EF}^{n+1})(1+C\ln\frac{\dot{\varepsilon_s}}{\dot{\varepsilon_0}}) \qquad \text{Eq.4}$$

In which $\varepsilon_{EF} = 2\ \varepsilon_{AB}$ and β is evaluated atT_{AB}.

To evaluate the proportion of the heat conducted into the work material β Non dimensional Thermal number need to be introduced as

$$R_t = \frac{\rho C_p U t_1}{K}$$ Eq.5

If $0.04 <= R_t \tan\phi <= 10$ then $\beta = 0.5 - 0.35 \log(R_t \tan\phi)$ Eq.6

Else $\beta = 0.3 - 0.15 \log(R_t \tan\phi)$ Eq.7

4.4 Calculation of the Shear Force along the primary Shear Plane

The deformation energy per unit volume w can be calculated by integrating the Total strain energy as;

$$w = \int_0^{\varepsilon_{EF}} \sigma \, d\varepsilon = \frac{\int_{T_w}^{T_{EF}} \rho \, C_p T \, dT}{(1-\beta)}$$

Shear Force F_s and Shear Stress τ_s can be obtained as,

$$F_s = \frac{w U t_1 b_1}{V_s} \qquad \tau_s = \frac{F_s}{A_s} = \frac{w U t_1}{V_s L}$$ Eq.8

The angle between the Resultant Force and the direction of the Primary Shear Zone can be obtained by using known Pressure distribution and Shear stress along the Shear Plane as;

$$\theta = \tan^{-1}[1 + 2\left(\frac{\pi}{4} - \phi\right) - \frac{c\,(K_u - K_l)}{2\,\tau_s}]$$ Eq.9

Where,

$$K_u = \frac{\sigma_1}{\sqrt{3}} \qquad \sigma_1 = (A + B\varepsilon_{AB}^n)(1 + C\ln(\frac{\varepsilon_s}{\varepsilon_o}))\,(1 - (\frac{T_{AB} - T_w}{T_m - T_w})^m)$$ Eq.10

$$K_l = \frac{\sigma_2}{\sqrt{3}} \qquad \sigma_2 = (A + B\varepsilon_{EF}^n)(1 + C\ln(\frac{\varepsilon_s}{\varepsilon_o}))\,(1 - \left(\frac{T_{EF} - T_w}{T_m - T_w}\right)^m)$$ Eq.11

4.5 Temperature Increase at Tool Chip Interface

The equation for increase in the temperature at tool chip interface is obtained by the Stevenson and Oxley [15] which is result of Boothroyd's numerical calculation. The ratio of maximum temperature increase at tool chip interface ($\Delta\theta_m$) to mean temperature increase of the chip ($\Delta\theta_c$) as

$$\frac{\Delta\theta_m}{\Delta\theta_c} = 0.06 - 0.195\,\delta(\frac{R_t\, t_2}{H})^{0.5} + 0.5\log(\frac{R_t\, t_2}{H})$$ Eq.12

Where, $\Delta\theta_c = \frac{F \sin\phi}{\rho\, C_p t_1 b_1 Cos\,(\phi - \alpha)}$

The average temperature at the tool chip interface can be calculated by using a constant ψ

$$T_{avg} = T_{EF} + \psi\,\Delta\theta_m$$ Eq.13

Hu et al. [16] suggested that if the equivalent cutting edge geometry is known the same procedure is adopted for a single straight cutting edge in oblique machining using the following experimental observations:

1. For a given normal rake angle and other cutting conditions, the force component in the direction of cutting, F_c and the force component normal to the direction of cutting and machined surface, F_T are nearly independent of the cutting edge inclination angle.

   So, $F_c = \frac{F_S \cos(\theta - \phi)}{\cos\theta}$

   $$F_T = \frac{F_S \sin(\theta - \phi)}{\cos\theta}$$ Eq.14

2. The Chip flow direction satisfies stabler's flow rule over a wide range of cutting conditions, if this rule is written in relation to the equivalent cutting edge, i.e.,

   $$\eta_c = i$$ Eq.15

The Resultant ForceF_R, the force normal to the F_C and F_T which results from a non zero inclination angle described by following equation as

$$F_R = \frac{F_c\left(\sin i - \cos i \sin\alpha_n \tan\eta_c\right) - F_T \cos\alpha_n \tan\eta_c}{\sin i \sin\alpha_n \tan\eta_c + \cos i}$$ Eq.16

The Force Components F_T and F_R do not act in the feed and radial directions. Therefore, the force components are redefined asP_1, P_2 and P_3, of which the positive directions are taken as the Velocity, negative Feed and radially outward directions.

For the equivalent cutting edge these are given by the following equations

$$P_1 = F_C \quad \text{Eq.17}$$

$$P_2 = F_T \cos C_s + F_R \sin C_s \quad \text{Eq.18}$$

$$P_3 = F_T \sin C_s - F_R \cos C_s \quad \text{Eq.19}$$

But, for the high approach angle, it is very difficult to predict for the radial thrust force, as suggested by Arseculeratne et al. [17] P3 can be calculated as;

$$P_3 = P_2 \tan(90 - (C_s - \Omega)) \quad \text{Eq.20}$$

here, P_1 = Main cutting force, N

P_2 = Axial thrust force, N

P_3 = Radial thrust force, N

5 Algorithm for Cutting force calculation

An iterative numerical scheme is combined and solved for the above equations over possible values of process parameters. The algorithm is shown in Fig. 4 which is solved iteratively by MATLAB.

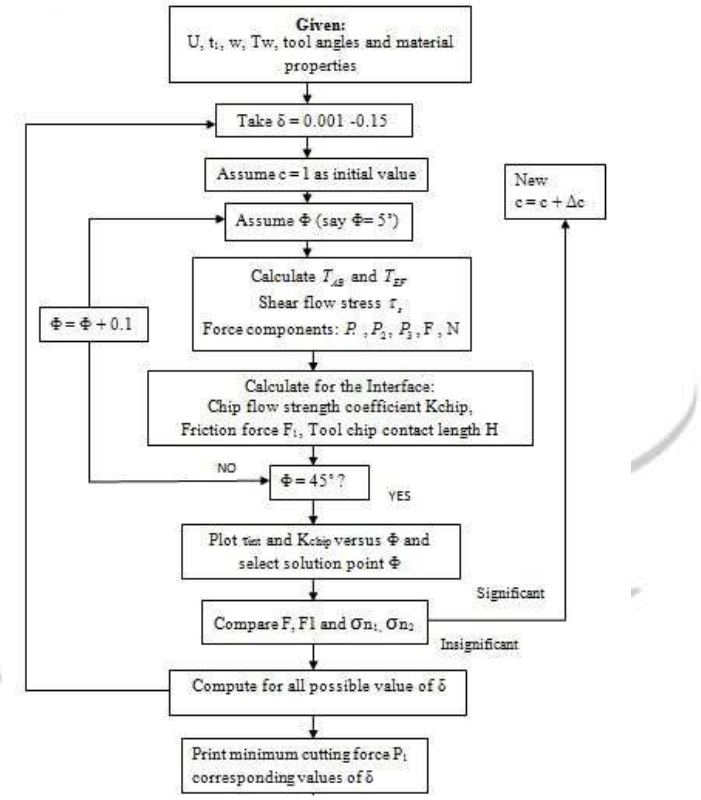

Fig.4 Algorithm for friction force modeling

6. Simulations and experimental validation

Experimental data are taken from Pankaj Rathod et al. [18]for validation.

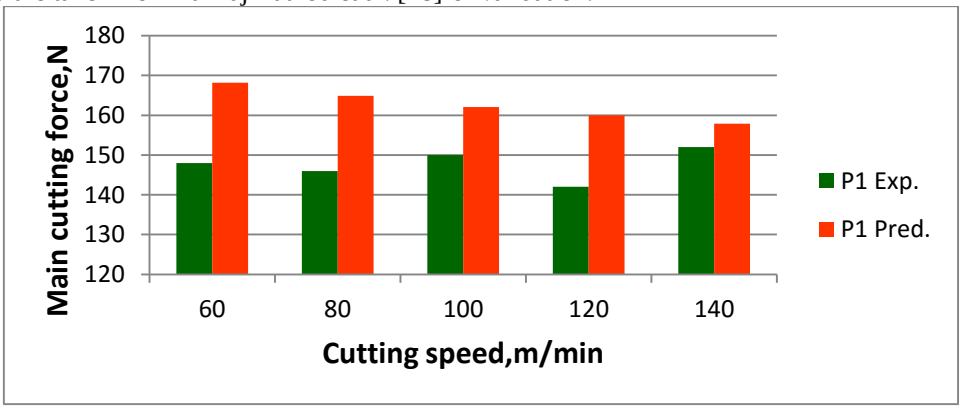

Fig.5 Main cutting force v/s cutting speed (feed=0.1mm/rev, depth of cut=0.5mm)

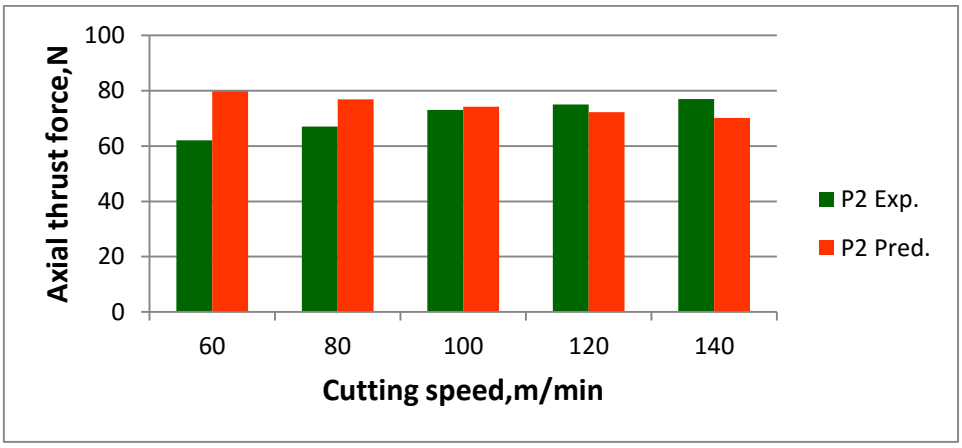

Fig.6 Axial thrust force v/s cutting speed (feed=0.1mm/rev, depth of cut=0.5mm)

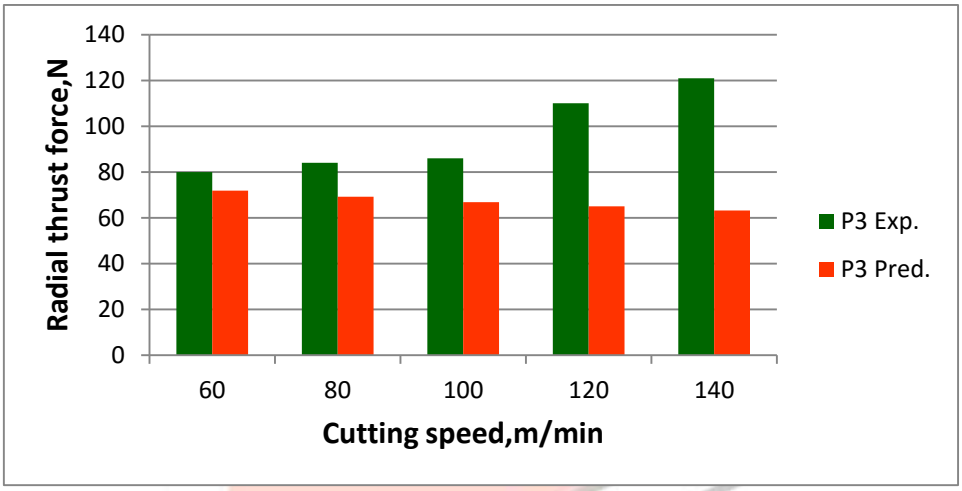

Fig.7 Radial thrust force v/s cutting speed (feed=0.1mm/rev, depth of cut=0.5mm)

6. CONCLUSION

- The titanium alloy Ti6Al4V is very difficult to machine and machinability criteria like; cutting force, friction force, surface roughness and tool life etc are very important parameters to consider.
- From the results it can be observed that for the Main cutting force plays an important role for the machining. Main cutting force and axial thrust force with varying speeds are in very good agreement with the experimental data.
- Created Model underestimates the radial thrust force. The reason behind that the due to low modulus of elasticity of the Ti6Al4V radial force amplitude increases suddenly. The effect of this phenomenon is very difficult to consider.
- Oxley has developed a mathematical calculation for carbon steel. but here oxley's model has extended to use for Titanium alloy Ti6Al4V. It proves the potentiality of oxley's approach to use different materials.

REFERENCES

[1] Ranga Komanduri and Zhen Bing Hou," On Thermoplastic Shear Instability in the Machining of a Titanium Alloy (Ti-6Al-4V)", Mettlurgical and Material Transactions, vol.33A, 2002.

[2] E.O.Ezugwu, J Bonney,Y.Yamane,"An overview of the machinability of aeroengine alloys", *Journals of material processing Technology*, vol.134, pp.233-253,2003.

[3] D. C. Drucker, "An Analysis of the Mechanics of Metal Cutting", *Journal of applied physics*, vol.20,1949.

[4] H T Young , P. Mathew, P L B Oxley, "Allowing for nose radius effects in predicting the chip flow direction and cutting forces in bar turning ", *Journal of Mechanical Engineering science*,1987.

[5] A Vyas, M C Shaw, " Mechanics of Saw-Tooth Chip Formation in Metal Cutting", *Journal of Manufacturing Science and Engineering*, vol.121,1999.

[6] J. Wang,"Development of a chip flow model for turning operations", *International Journal of Machine Tools & Manufacture*, vol. 41, pp.1265–1274, 2001.

[7] Jiang Hua,Rajiv Shivpuri," Prediction of chip morphology and segmentation during the machining of Titanium alloys", *Journal of Materials Processing Technology*, vol.150, pp.124–133,2004.

[8] S.A.Iqbal, P.T.Mativenga, M.A.Sheikh, "A comparative study of the tool–chip contact length in turning of two

engineering alloys for a wide range of cutting speeds", *Int. Journals for Advance Manufacturing Technology*, vol.42,pp.30-40,2009.

[9] Mohammad Sima,Tugrul Ozel," Modified material constitutive models for serrated chip formation simulations and experimental validation in machining of Titanium Alloy Ti–6Al–4V ", *International Journal of Machine Tools & Manufacture*, Vol. 50, pp. 943–960, 2010.

[10] Guang Chen, Chengzu Ren, Xiaoyong Yang , Xinmin Jin, Tao Guo "Finite element simulation of high-speed machining of titanium alloy (Ti–6Al–4V) based on ductile failure model",*Int. Journals for Advance Manufacturing Technology*,vol.56,pp.1027-1038,2011.

[11] M. Calamaz & D. Coupard & M. Nouari & F. Girot," Numerical analysis of chip formation and shear localisation processes in machining the Ti-6Al-4V titanium alloy", *Int. Journals of Advance Manufacturing Technology*, vol.53,pp.887-895,2011.

[12] Oxley L.B "An Analytical Approach to Assessing Machinability", The Mechanics of Machining, E. Horwood, Chichester, England. (1989)

[13] Tugrul Ozel and Mohhamad Sima,"Finite element simlation of high speed machining Ti6Al4V alloy using modified material models".*Transactions of NAMRI/SME,*Vol.38,2010.

[14] Amir H.,Adibi-Sedeh, "Extension of Oxley's Analysis of Machining to Use Different Material Models", Transactions of the ASME Vol. 125, pp. 656-666, November 2003.

[15] Stevenson, M. G., and Oxley, P. L. B, ''An Experimental Investigation of the Influence of Speed and Scale on the Strain-Rate in a Zone of Intense Plastic Deformation'', Proc. Inst. Mech. Eng., 184~31 pp.561–576.,(1969-1970).

[16] R S Hu, P Mathew, P L B Oxley and H T Young,"Allowing for end cutting edge effects in predicting forces in bar turning with oblique machining conditions", *proc.Instn. mech engrs,*Vol. 200 No. C2,1986.

[17] S.D.J.A.Arsecularatne, G. Barrow, S. Hinduja ,"Prediction of the radial force in turning using feed force data",*int.J.Mach.Tools manufacturing,Vol.33, pp.827-839,1993.*

[18] Pankaj Rathod,Sivanandam,Aravindan,Venkateswara Rao Puruchuri, "Evaluating the effectiveness of the novel surface textured tools in enhancing the machinability of titanium alloy (Ti6Al4V) ", *Journal of Advanced Mechanical Design, Systems, and Manufacturing*,Vol. 9,No.3,2015.

[a] www.asm.matweb.com

List of Symbols

Symbol	Symbol name
A	yield strength in the Johnson-Cook material model
As	area of the primary shear zone
B	strength coefficient in the Johnson-Cook material model
C	strain rate constant in the Johnson-Cook material model
c	Strain rate in oxley's model
Cp	specific heat of work material
F	friction force at the tool-chip interface
Fs	shear force along the nominal shear plane
H or Lc	length of contact between tool and chip
k_l	shear strength at the lower boundary of the primary shear zone
k_u	shear strength at the upper boundary of the primary shear zone
k_{chip}	shear strength at the tool-chip interface obtained from the material model
L	length of the shear plane
m	temperature exponent in the Johnson-Cook material model
N	normal force at the tool-chip interface
n	strain hardening exponent in Oxley's and the Johnson-Cook material models
p_A	hydrostatic pressure at the free surface of the nominal shear plane

p_B	hydrostatic pressure at the tool tip
R_T	thermal number of work material
$Tavg$	average temperature at the tool-chip interface
T_M	melting temperature
T_r	reference temperature
T_w	temperature of the uncut work material
t_1	undeformed chip thickness
t_2	chip thickness
U	Cutting velocity
Vs	shear velocity
Vc	chip velocity
α	Orthogonal rake angle
δ	the ratio of the secondary shear zone thickness to the chip thickness
ε_{AB}	strain at the midplane of the primary shear zone
ε_{EF}	strain at the upper boundary of the primary shear zone
$\acute{\varepsilon}$	strain rate
$\acute{\varepsilon}_0$	reference strain rate
$\acute{\varepsilon}_s$	strain rate in the primary shear zone
Φ	Shear plane angle
θ	the angle of the resultant force on the shear plane with respect to the shear plane direction
σ	flow stress
ψ	a constant calibration factor equal to the ratio of the average temperature increase to the maximum temperature rise at the tool-chip interface
τ_{int}	shear strength at the tool-chip interface obtained from equilibrium